Aqueous Mediated Synthesis of Mesostructured Manganese Germanium Sulfide with Hexagonal Order

K. Kasthuri Rangan,[†] Simon J. L. Billinge,[‡] Valeri Petkov,[‡] Joy Heising,[†] and Mercouri G. Kanatzidis*,[†]

Departments of Chemistry and of Physics and Astronomy and Center for Fundamental Materials Research, Michigan State University, East Lansing, Michigan 48824

Received July 20, 1999

Research on the self-assembly of inorganic clusters around organized sets of organic molecules is of great interest, primarily because of the valuable lessons which could be learned for materials design and due to the potential high impact materials so designed could have in technology.[1] Incorporation of electrical properties into nano- and mesostructured materials presents a special challenge, because non-oxidic building blocks have to be employed and, at the same time a great opportunity, because new functionality could be expected in these systems.[2] Synthesis of mesostructured silicates by the Mobil group[3] showed a way to achieve tunable ordered structures in the mesoscale using surfactants as templating agents. These materials are promising for applications in catalysis,[4] but lack potential as optical or electronic materials. Our effort is to incorporate electronic properties into nano- and mesostructured materials. The report of the synthesis of microstructured metal sulfides[5] stimulated the preparation of a number of metal sulfides with *microstructured* open framework structures.[6] This was followed by reports on the synthesis of *mesostructured* CdS,[7] SnS,[8] and ZnS[9] with the incorporation of cationic surfactants. In addition, the hydrothermal treatment of amorphous GeS_2 and cetyltrimethylammonium bromide was reported to give lamellar mesostructured GeS_x phases.[10] Recently, MacLachlan et al. reported the supramolecular assembly of mesostructured metal germanium sulfides from $Ge_4S_{10}^{4-}$ clusters.[11] They have emphasized the need for nonaqueous solvent formamide, playing a key role in their synthesis of hexagonal ordered phase. The reported phases claimed to have flexible and adjustable composition. Indepentendly, we focused our efforts on the self-assembly of $Ge_4S_{10}^{4-}$ adamantane ions[12] with surfactant micelles in *aqueous medium* and have prepared mesostructured materials $[C_nH_{2n+1}N(CH_3)_3]_2MGe_4S_{10}$ (C_nMGeS) with divalent metal ions with divalent metal ions Zn^{2+}, Cd^{2+}, Hg^{2+}, Ni^{2+}, and Co^{2+}. These materials are different from those of MacLachlan et al. and contain pores resembling wormholes.[13] During our investigation, we observed reactions with Mn^{2+} ions in aqueous medium behaved differently and did not result in an immediate precipitation as with the other divalent metal ions. Subsequently, we carried out reactions with Mn^{2+} ions under hydrothermal conditions and discovered a new mesostructured phase of $MnGe_4S_{10}$ with hexagonally ordered pores with mesityltrimethylammonium surfactant.

$[C_{14}H_{29}N(CH_3)_3]_2MnGe_4S_{10}$ (C_{14}MnGeS) was synthesized by reacting a mixture of $Na_4Ge_4S_{10}$, $MnCl_2{\cdot}4H_2O$, and mesityltrimethylammonium bromide in a stoichiometric ratio 1:1:2, at 120 °C under hydrothermal conditions.[14] The reaction could be expressed by the following

$$Na_4Ge_4S_{10} + MnCl_2 + 2C_{14}H_{29}N(CH_3)_3Br \rightarrow [C_{14}H_{29}N(CH_3)_3]_2MnGe_4S_{10} + 2NaCl + 2NaBr \quad (1)$$

From elemental analysis, the Mn:Ge:S ratio was found to be 1:4:10.[15] Elemental analysis also confirmed the absence of sodium or bromide ions in the sample. The thermal gravimetric (TG) analysis showed a weight loss of 43.47% from 180 °C to 500 °C,[16] which corresponds to a loss of two moles of the surfactant (43.30% calcu-

[†] Department of Chemistry and Center for Fundamental Materials Research.

[‡] Department of Physics and Astronomy and Center for Fundamental Materials Research.

(1) (a) *Modular Chemistry,* Michl, J., Ed.; Kluwer Academic Publishers: Netherlands, 1997. (b) Yaghi, O. M.; Li, H.; Davis, C.; Richardson, D.; Groy, T. L. *Acc. Chem. Res.* **1998**, *31*, 474−484.

(2) (a) Imry, Y. *Introduction to Mesoscopic Physics*; Oxford University Press: New York, 1997. (b) Schmid, G.; Bäumle, M.; Geerkens, M.; Heim, I.; Osemann, C.; Sawitowski, T. *Chem. Soc. Rev.* **1999**, *28*, 179−185.

(3) (a) Kresge, C. T.; Leonowicz, M. E.; Roth, W. J.; Vartuli, J. C.; Beck, J. S. *Nature* **1992**, *359*, 710−712. (b) Beck, J. S.; Vartuli, J. C.; Roth, W. J.; Leonowicz, M. E.; Kresge, C. T.; Schmitt, K. D.; Chu, C. T.-W.; Olson, D. H.; Sheppard, E. W.; McCullen, S. B.; Higgins, J. B.; Schlenker, J. L. *J. Am. Chem. Soc.* **1992**, *114*, 10834−10843.

(4) Corma, A. *Chem. Rev.* **1997**, *97*, 2373−2419.

(5) Bedard, R. L.; Wilson, S. T.; Vail, L. D.; Bennett, E. M.; Flanigen, E. M. *Zeolites: Facts, Figures, Future*; Jacobs, P. A., van Santen, R. A., Eds.; Elsevier Science Publishers B. V.: Amsterdam, Netherlands, 1989; p 375.

(6) (a) Yaghi, O. M.; Sun, Z.; Richardson, D. A.; Groy, T. L. *J. Am. Chem. Soc.* **1994**, *116*, 807−808. (b) Parise, J. B. *Science* **1991**, *251*, 293−294. (c) Dhingra, S.; Kanatzidis, M. G. *Science* **1992**, *258*, 1769. (d) Kim, K.-W.; Kanatzidis, M. G. *J. Am. Chem. Soc.* **1992**, *114*, 4878. (e) Kim, K. W.; Kanatzidis, M. G. *J. Am. Chem. Soc.* **1998**, *120*, 8124−8135.

(7) (a) Braun, P. V.; Osenar, P.; Stupp, S. I. *Nature* **1996**, *380*, 325−328. (b) Stupp, S. I.; Braun, P. V. *Science* **1997**, *277*, 1242−1248.

(8) (a) Ozin, G. A. *Supramol. Chem.* **1995**, *6*, 125−134. (b) Jiang, T.; Ozin, G. A. *J. Mater. Chem.* **1998**, *8*, 1099−1108. (c) Jiang, T.; Ozin, G. A.; Bedard, R. L. *J. Mater. Chem.* **1998**, *8*, 1641−1648. (d) Li, J. Q.; Kessler, H. *Microporous Mater.* **1997**, *9*, 141−147. (e) Li, J. Q.; Kessler, H.; Delmotte, L. *J. Chem. Soc., Faraday Trans.* **1997**, *93*, 665−668. (f) Li, J. Q.; Delmotte, L.; Kessler, H. *J. Chem. Soc., Chem. Commun.* **1996**, 1023−1024.

(9) Li, J.; Kessler, H.; Soulard, M.; Khouchaf L.; Tuiler, M.-H. *Adv. Mater.* **1998**, *10*, 946.

(10) Fröba, M.; Oberender, N. *J. Chem. Soc., Chem. Commun.* **1997**, 1729−1730.

(11) MacLachlan, M. J.; Coombs, N.; Ozin, G. A. *Nature* **1999**, *397*, 681−684.

(12) Bonhomme, F.; Kanatzidis, M. G. *Chem. Mater.* **1998**, *10*, 1153−1159.

(13) Wachhold, M.; Rangan, K. K.; Billinge, S. J. L.; Petkov, V.; Heising, J.; Kanatzidis, M. G. Submitted for publication.

(14) A total of 1.40 g $Na_4Ge_4S_{10}$ (2 mmol), 0.39 g $MnCl_2{\cdot}4H_2O$ (2 mmol), and 1.34 g $C_{14}H_{29}N(CH_3)_3Br$ (4 mmol) were mixed with 3 mL of distilled water in a Pyrex tube (13 mm o.d., 10 cm length). The tube was evacuated, flame sealed, and heated at 120 °C for 4 days. The yellow product formed was separated and washed with ethanol/water (5:1 by volume) mixture and acetone and dried under vacuum. C,H,N analysis (Perkin-Elmer 2400 CHNS/O analyzer) gave C, 32.05%, H, 6.65%, and N, 2.57% (expected C, 34.64%, H, 6.49%, and N, 2.38%).

(15) Semiquantitative microprobe analyses were performed using a JEOL JSM-35C scanning electron microscope equipped with a Tracor Northern energy dispersive spectroscopy (EDS) detector. Data acquisition was performed several times in different areas of the samples with an accelerating voltage of 20 kV and 30−35 s accumulation time.

10.1021/cm990456j CCC: $18.00 © 1999 American Chemical Society
Published on Web 09/16/1999

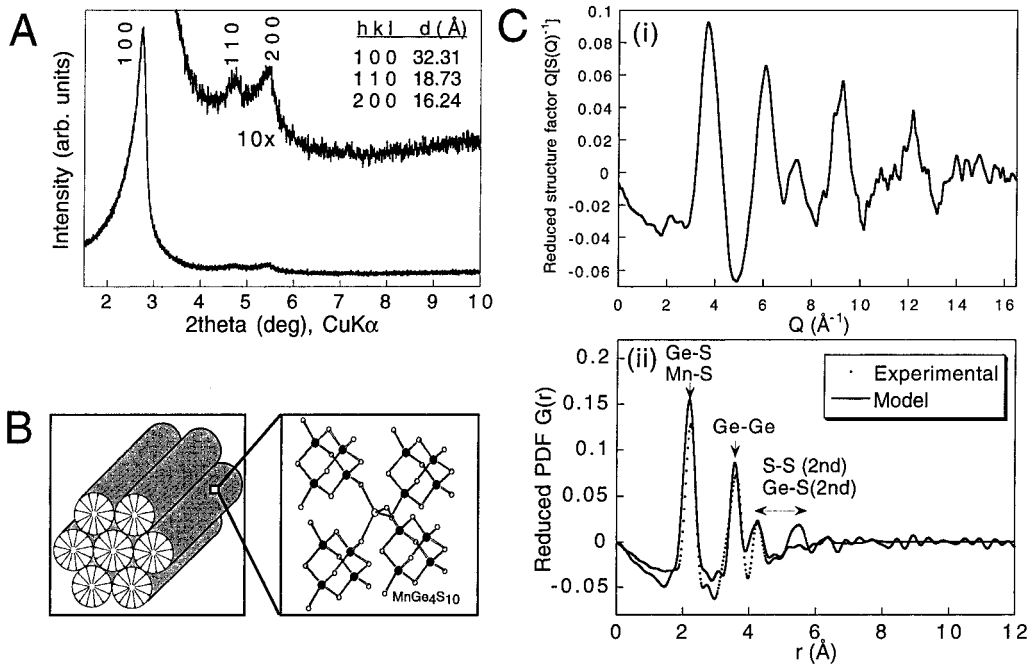

Figure 1. (A) Powder X-ray diffraction pattern of $C_{14}MnGeS$ (Rigaku, Cu Kα) showing low angle peak corresponding to 100 of the hexagonal cell and 110 and 200 reflections in an expanded scale, (B) schematic representation of hexagonal ordered structure of $C_{14}MnGeS$ and local structure of "metal−thiogermanate wall" encapsulating rod micelles, and (C) (i) reduced structure factors $Q[S(Q) - 1]$ of $C_{14}MnGeS$, derived from the wide-angle X-ray diffraction pattern (Huber diffractometer in symmetric reflection geometry and Ag K_α radiation) and (ii) reduced pair distribution function, $G(r)$ plotted against distance r. Figure also shows PDFs corresponding to a model based on the structure of crystalline $[(CH_3)_4N]_2MnGe_4S_{10}$.

lated). There is no weight loss observed below 180 °C, indicating the absence of any water molecules in the compound. Further, C,H,N analyses also support the TG analysis.[14]

The powder X-ray diffraction pattern of $C_{14}MnGeS$ is shown in Figure 1A. It is very similar to those of the hexagonal phases reported for mesoporous silica.[3] We could index the three reflections at 32.31, 18.73, and 16.24 Å as 100, 110, and 200, respectively, with hexagonal lattice parameter, $a_H = 37.31$ Å. As with other mesostructured oxidic phases,[3] we do not observe any Bragg diffraction peaks at wide angle, suggesting that the $MnGe_4S_{10}$ framework (that is the walls) lacks long range order. Nevertheless, these materials exhibit well-defined diffuse scattering at $2\theta > 10°$, consistent with the presence of short-range local order and nonperiodic wall structure. On the basis of the X-ray diffraction pattern, the mesopores in $C_{14}MnGeS$ are hexagonally packed and embedded in a three-dimensional $MnGe_4S_{10}$ framework as shown schematically in Figure 1B.

To probe the local structure of the amorphous manganese germanium sulfide framework, we analyzed the X-ray diffuse scattering with the atom pair distribution function (PDF) technique.[17] Figure 1C(i) shows the reduced structure factor $Q[S(Q)^{-1}]$ of $C_{14}MnGeS$ obtained from the powder diffraction data.[18] The corresponding pair distribution functions derived from the structure factor Q are shown in Figure 1C(ii).[18] Characteristic atom pairs are assigned corresponding to the strong peaks in the PDF (Figure 1C(ii)). The PDF shows that there is well-defined local order as seen by the presence of interatomic correlation vectors at 2.2 and 3.8 Å which correspond to Ge−S and Ge−Ge distances in the $[Ge_4S_{10}]^{4-}$cluster. The structural origin of these correlation vectors is consistent with the presence of $[MnGe_4S_{10}]^{2-}$structural modules. The results agree well with the PDFs calculated from the model developed on

(16) TGA data were obtained with a computer-controlled Shimadzu TGA-50 thermal analyzer. Typically 25 mg of sample were placed in a quartz bucket and heated in a nitrogen flow of 50 mL/min with a rate of 2 °C/min.

(17) An overview of the use of this and other scattering techniques for studying disordered materials is given in: Billinge, S. J. L. *Curr. Opin. Solid State Mater. Sci.* **1996**, *1*, 477.

(18) The XRD data for the pair distribution function (PDF) determination were collected independently using a Huber diffractometer in symmetric reflection geometry (up to $2\theta_{max} = 140°$) and Ag Kα radiation ($\lambda = 0.5609$ Å). The PDF was obtained using standard methods. The data were corrected for background, absorption, polarization, Compton and multiple scattering and normalized by the incident flux, the number of scatterers, and the average atomic form factor of the sample to obtain the normalized total scattering function $S(Q)$ ($Q = 4\pi \sin\theta/\lambda$ where 2θ is the scattering angle). The reduced radial distribution function, or pair distribution function (PDF) $G(r)$, is obtained from $S(Q)$ through a Fourier transform: $G(r) = [4\pi r\rho(r) - 4\pi r\rho_0] = (2/\pi)\int_0^\infty Q[S(Q) - 1]\sin(Qr)\,dQ$. Where $\rho(r)$ is the atomic pair density function. The function $G(r)$ represents the radial density distribution showing peaks at distances, r, which separate pairs of atoms in the solid. For example, the first strong peak occurs at $r \approx 2.2$ Å corresponding to the Ge−S nearest neighbor peak in these materials. It is a measure of the short-range atomic order in the solid and does not presume any crystallinity. The procedures used to perform atomic pair distribution function analysis of XRD data have been published elsewhere [Egami, T. *Mater. Trans. JIM* **1990**, *31*, 163. Billinge, S. J. L.; Egami, T. *Phys. Rev. B* **1993,** *47*, 14386].

(19) Achak, O.; Pivan, J. Y.; Maunaye, M.; Loüer, M.; Loüer, D. *J. Alloys Compd.* **1995**, *219*, 111−115.

(20) The $G(r)$ function was calculated based on the crystalline analogue model $[(CH_3)_4N]_2MnGe_4S_{10}$ (ref 6a) with some modifications to allow for the periodic structural disorder present in the samples. The PDF was calculated using a locally written program, RESPAR, which calculates $G(r)$ from a given crystalline structure. Static and thermal disorder is incorporated by broadening PDF peaks with Gaussians.

(21) Raman spectra of the samples were recorded on a Holoprobe Raman spectrograph equipped with a 633 nm helium−neon laser and a CCD camera detector. Infrared spectra of far-IR region (600−100 cm^{-1}) were recorded (CsI pressed pellets) with a computer-controlled Nicolet 750 Magna-IR Series II spectrometer equipped with a TGS/PE detector and a silicon beam splitter in 2 cm^{-1} resolution.

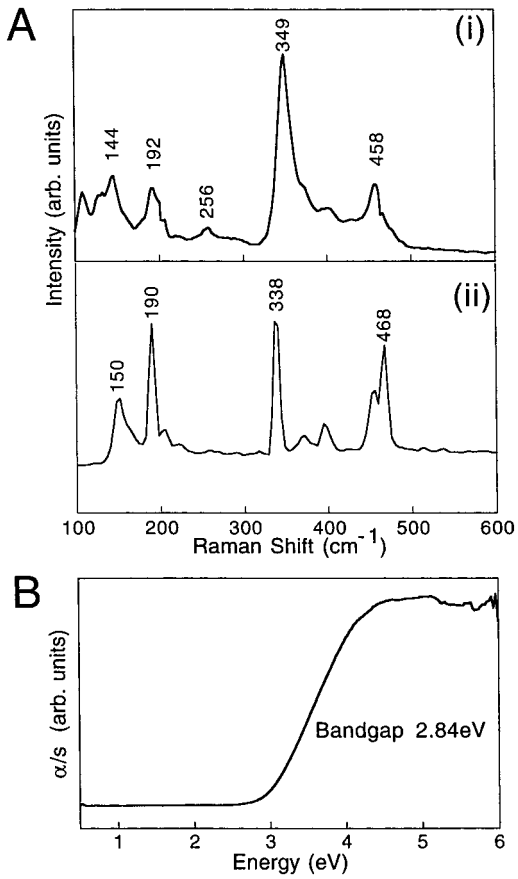

Figure 2. (A) Raman spectra of (i) $C_{14}MnGeS$ showing characteristic peaks corresponding to adamentane Ge_4S_{10} unit and Mn−S stretching and (ii) $C_{14}GeS$, lamellar phase containing isolated $Ge_4S_{10}^{4-}$ clusters, and (B) solid-state absorption spectrum of $C_{14}MnGeS$.

the basis of the crystalline analogue $[(CH_3)_4N]_2MnGe_4S_{10}$.[6a,19,20] Furthermore, the peak corresponding to the Mn−S pair (bond distance of 2.4 Å) is most likely overlapping with the peak at 2.2 Å. There is no structural coherence above 10 Å observable, (Figure 1C(ii)) which would be approximately the Mn−Mn separation. This suggests that the long-range order is destroyed because the lack of well-defined orientational relationship between neighboring adamantoid ions.

The three-dimensional nature of the framework is further supported by differential scanning calorimetric (DSC) analysis. It is a general observation that the lamellar phases show a phase transition well below their decomposition temperature, due to "melting" or conformational changes of the long alkyl chains of the surfactant molecules in the intralamellar space. For example, the parent phase, $[C_{14}H_{29}N(CH_3)_3]_4Ge_4S_{10}$ ($C_{14}GeS$) shows a phase transition around 150 °C.[12] $C_{14}MnGeS$ does not show any such phase transition below 180 °C, indicative of the three-dimensional nature of the framework. From 180 to 220 °C, an endothermic peak occurs, corresponding to the decomposition of the surfactants. The framework collapsed on complete removal of the surfactant at 500 °C, leading to an amorphous final product.

The Raman spectrum of the $C_{14}MnGeS$ and the corresponding lamellar parent $C_{14}GeS$[12] which has isolated $Ge_4S_{10}^{4-}$ clusters, are shown in Figure 2A.[21] As compared to the lamellar phase, mainly the peak at 458 cm^{-1} in $C_{14}MnGeS$, corresponding to terminal $Ge-S_{term}$ symmetric stretching mode, is affected in intensity and shifted to lower frequency. The peak at 349 cm^{-1} corresponds to the totally symmetric breathing vibrational mode of the inner cage Ge_4S_6 is not affected in intensity, although shifted to higher frequency as compared to isolated $Ge_4S_{10}^{4-}$ clusters.[22] Further, the peak at 256 cm^{-1} could be assigned to Mn−S stretching which is absent in the lamellar phase. The far-IR spectrum showed characteristic broad bands at 423, 377, 279, and 197 cm^{-1}, corresponding to the adamantane $Ge_4S_{10}^{4-}$ cluster and is similar to that of $[(CH_3)_4N]_2MnGe_4S_{10}$.[23] The band centered at 423 cm^{-1} due to $Ge-S_{term}$ stretching is shifted to lower frequency as compared to compounds with isolated $Ge_4S_{10}^{4-}$ anions (458 cm^{-1}). Thus it is clear that the terminal S atom of the adamantane cluster is bonded to Mn.

Finally, a high-resolution transmission electron (HR-TEM) micrograph[24] of $C_{14}MnGeS$ is consistent with the rod micellar structure encapsulated by metal thiogermanate walls. Figure 3A shows the tubular arrangement of the pores filled with rodlike surfactant micelles The distance between the pores is ∼30 Å, close to the values obtained from powder X-ray diffraction pattern (Figure 1A). We were able to remove up to 60% of the surfactant by "calcination" at 180 °C for 2 h under dynamic vacuum without framework collapse. The powder X-ray diffraction pattern of the "calcined" sample

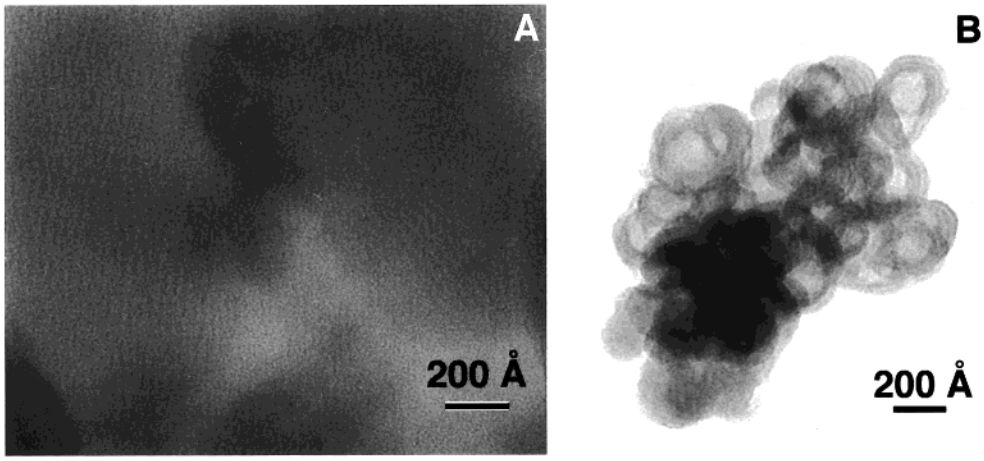

Figure 3. High-resolution transmission electron micrographs of $C_{14}MnGeS$ (A) as prepared sample and (B) "calcined" sample.

showed a low-angle peak at 30 Å, with a decrease of ~2 Å from the "as prepared" sample suggesting that the integrity of the framework is retained in the sample. A TEM micrograph of the "calcined" phase is given in Figure 3B where vesicular-like structures are clearly visible.

The property that distinguishes the metal sulfide frameworks from those of silica, is the much narrower optical energy band gap of the former. Indeed C_{14}MnGeS possesses a well-defined sharp optical absorption associated with band gap of 2.84 eV[25] (Figure 2B), which is in the range suitable for optoelectronic applications.

In conclusion, we have shown here that it is possible to self-assemble adamantane $Ge_4S_{10}^{4-}$ clusters in aqueous medium and form hexagonally ordered mesostructures by employing the hydrothermal method of synthesis. We were also able to synthesize similar phases with the $C_{12}H_{25}N(CH_3)_3Br$, $C_{16}H_{33}N(CH_3)_3Br$, and $C_{18}H_{37}N(CH_3)_3Br$ surfactants thereby "tuning" the pore size. The pattern as observed from the powder X-ray diffraction pattern showed a corresponding increase with increase in surfactant chain length.

Acknowledgment. Financial support from the National Science Foundation CHE 96-33798, (Chemistry Research Group) is gratefully acknowledged. This work made use of the SEM and TEM facilities of the Center for Electron Optics, Michigan State University. We acknowledge the use of the W.M. Keck Microfabrication Facility at Michigan State University, a NSF MRSEC facility.

CM990456J

(22) (a) Campbell, J.; DiCiommo, D. P.; Mercier, H. P. A.; Pirani, A. M.; Schrobilgen, G. J.; Willuhn, M. *Inorg. Chem*. **1995**, *34*, 6265−6272. (b) Muller, A.; Cyvin, B. N.; Cyvin, S. J.; Pohl, S.; Krebs, B. *Spectrochim. Acta* **1976**, *32A*, 67−74.

(23) Achak, O.; Pivan, J. Y.; Maunaye, M.; Loüer, M.; Loüer, D. *J. Solid State Chem*. **1996**, *121*, 473−478.

(24) High-resolution transmission electron micrographs were acquired with a JEOL 120CX instrument equipped with a CeB_6 filament and operating at 120 kV. A carbon-supported copper grid was dipped in the dry powder or a suspension of the sample in hexane.

(25) Energy gaps were obtained as described in: McCarthy, T. J.; Ngeyi, S.-P.; Liao, J.-H.; DeGroot, D. C.; Hogan, T.; Kannewurf, C. R.; Kanatzidis, M. G. *Chem. Mater*. **1993**, *5*, 331.